

**ENHANCED PHOTOCATALYTIC  
DEGRADATION OF BISPHENOL A UNDER  
VISIBLE LIGHT IRRADIATION USING NANO  
DISC RICE HUSK ASH SILICA-TEMPLATED  
OXYGEN DOPED MESOPOROUS CARBON  
NITRIDE AND CARBON DOTS MODIFIED  
GRAPHITIC CARBON NITRIDE**

**SHITTU FATIMAH BUKOLA**

**UNIVERSITI SAINS MALAYSIA**

**2021**

**ENHANCED PHOTOCATALYTIC  
DEGRADATION OF BISPHENOL A UNDER  
VISIBLE LIGHT IRRADIATION USING NANO  
DISC RICE HUSK ASH SILICA-TEMPLATED  
OXYGEN DOPED MESOPOROUS CARBON  
NITRIDE AND CARBON DOTS MODIFIED  
GRAPHITIC CARBON NITRIDE**

by

**SHITTU FATIMAH BUKOLA**

**Thesis submitted in fulfilment of the requirements**

**for the degree of**

**Doctor of Philosophy**

**December 2021**

## ACKNOWLEDGEMENT

In the name of Allah, the most Gracious, the most Merciful. All praise, adoration and gratitude belong to Almighty Allah for giving me the opportunity and making it possible for me to start and complete my PhD journey. And for the strength and perseverance He has given me throughout the journey, His blessings throughout my life and completion of this thesis, Alhamdulillah Robbil alamin. May the peace and blessings of Allah be upon our prophet Muhammad, who has taught us to live our lives according to his sunnah.

I would like to extend my sincere gratitude to my main supervisor, Dr Mohammad Anwar Mohamed Iqbal, for his insightful comments, continuous encouragement and advice, and solid support throughout my PhD journey. I admire your positive attitude and great passion on your work. I would also like to thank my co-supervisor, Assoc Prof. Dr Mohamad Nasir Mohamad Ibrahim, for his sincere suggestions, supportive advice and assistance to me for the work and future life. I would also like to appreciate Prof. Dr. Farook Adam for his guidance and suggestions. May Allah preserve you all upon goodness.

I would like to extend my appreciations to all the technical and administrative staff of School of Chemical sciences for making my work go smoothly, especially En. Azhar, En. Azizo, En. Ali, En. Siva, En. Zamri, En. Fauzan, En. Razly, En. Sujayendran and Puan Roziana, and not forgetting the technical staff of Science and Engineering Research Center (SERC) and Centre for Global Archeological Research, Universiti Sains Malaysia, for their support. My heartfelt appreciations to Assoc. Prof. Dr. Noor Hana Hanif Abu Bakar of School of chemical sciences, Dr. Noor

Fatimah of Advanced Medical and dental Institute (AMDI), and Puan Hariy (SERC), Universiti Sains Malaysia, for their support during my research application, LC-MS and XPS analysis, respectively. I greatly acknowledge the Ministry of Education Malaysia (Higher Education) for the fundamental Research Grant Scheme (FRGS/1/2019/STG01/USM/02/7). It has been a fundamental aspect of this research.

Furthermore, I would also like to greatly acknowledged all my friends and colleagues especially Halimah Sheu-Babamale, Rania Edrees, Dr. Suwaibatu Mamman, Nur Ruzaina, Nur Hanisah, Normawati Jasni, Dr. Umie Fatihah, Fatin Hazirah, Asma, Izzana, Najwa, Dr. Usman Saidu, Muhammad Faisal, Dr. Tan Kok, Dr. Abu Ahmad Ismail Adebayo, Dr Saheed Adewale (KSA), Dr Abdulsamad and Samirah Adebayo (Australia), Rofiat Bello-Mudashiru and family, Dr. Bilikisu Jimada-Ojuolape and family, Nusirat Gold and family, Dr. Kazeem AbdulRauf and family, Dr. Abdulrazaq Kayode and Mrs Saidat Olaniran. Special appreciation to Aminat Owodunni for the priceless efforts and sleepless nights during my thesis format arrangement. Thank you for your help, support and togetherness during my study. I will cherish the memorable days with you all.

My profound appreciation goes to my mother Alhaja Rafat Abimbola, brothers; Ismail Olatunji and Moshood Oyeyemi, sisters; Khawlat Oyeronke, Moshoodat Okikiola, Khadijah Opeyemi and Taoheedat Olabisi, and the entire Ibiyeye's family. Thank you for your prayers, support, and encouragement. Also, to my late Dad, Alhaji Moshood Oyeyemi Ibiyeye, I know you would be proud of me. May Allah be pleased with your soul and grant you al-jannatul firdaos. I would also like to express my appreciations to Pharm. Hazeemat Omolara Oyelola-Adeyemi, Dr. Mrs. Oyeleye Oyelola-Adedeji and bro. Deji Mustapha and family (NYC). Thank you for your endless encouragement, love and support.

I would like to appreciate my parents-in-law; Alhaji Murtadha Adedayo and Alhaja Hamdalah Adeitan Shittu, and the entire shittu's family especially hajia Kafilah Shola Shittu-Omowale, Sarat Niniola Omowale, Dr. Ruqayyah Omolaraeni Jimoh. Thank you for your prayers, love, and support. I am grateful to my sister-friends; Dr Mrs Taoheedah Alanamu-Ahmed, Dr Mrs Bashirah Labaika-Oloyin, Maryam Sulaiman-Asha Habibah Alege-Aduragba, Taofiqah Amoloye-Abu and Fatimah Segilola Abdulkadir. Thank you so much for all you do for me. May Allah bless you all.

I do not have words to express my feelings, profound and special appreciations to my husband Abdulkabir Oluwashina Abefe Shittu and my children; Al-Ameen Gbolahan Shittu, Muhsinah Morolake Shittu and Muhammad Iyiola Shittu. Thank you for your care, patience, prayers, unconditional support, absolute love, and your pursuit of my happiness and welfare. You gave me courage to face up all challenges in life. I love you so much and I will not trade you all for anything.

Finally, I am very grateful to The Federal Polytechnic Offa, for given me the opportunity to do my PhD program in Universiti sains Malaysia. My sincere gratitude goes to my colleagues; Hajia Jelilat Ibikunle, Mrs. Aminat Okunola, Mrs. Kemi Olawale-Adeyemi, Mrs. Tinuola Bakare-Aremu, Mr Abubakar, Mr Taofeek, Mr Girigisu, Mr Olaoye and the senior and junior colleagues in the department of SLT, School of Applied sciences, FEDPOFFA. Thank you so much. My special appreciation goes to the Tertiary Education Trust Fund (TETFund), Nigeria, for the scholarship awarded to me for this PhD program. May God bless Nigeria.

## TABLE OF CONTENTS

<b>ACKNOWLEDGEMENT.....</b>	<b>ii</b>
<b>TABLE OF CONTENTS.....</b>	<b>v</b>
<b>LIST OF TABLES .....</b>	<b>xiv</b>
<b>LIST OF FIGURES.....</b>	<b>xviii</b>
<b>LIST OF SYMBOLS.....</b>	<b>xxvi</b>
<b>LIST OF ABBREVIATIONS.....</b>	<b>xxvii</b>
<b>ABSTRAK .....</b>	<b>xxxi</b>
<b>ABSTRACT.....</b>	<b>xxxiii</b>
<b>CHAPTER 1 INTRODUCTION AND LITERATURE REVIEW .....</b>	<b>1</b>
1.1 Background .....	1
1.2 Literature Review .....	4
1.2.1 Water pollution and the environment.....	4
1.2.2 Toxic organic pollutants .....	6
1.2.2(a) Emerging Organic Contaminants (EOCs) .....	8
1.2.2(b) Endocrine Disrupting Compounds .....	10
1.2.3 Bisphenol A (BPA).....	12

1.2.3(a)	Sources of BPA.....	13
1.2.3(b)	Toxicity of BPA .....	15
1.2.4	Advanced Oxidation Processes for BPA Removal .....	23
1.2.5	Homogeneous photocatalysis.....	26
1.2.6	Heterogeneous photocatalysis.....	26
1.2.7	Graphitic Carbon Nitride .....	31
1.2.7(a)	Synthesis of g-C <sub>3</sub> N <sub>4</sub> .....	38
1.2.8	Mesoporous Carbon Nitride .....	41
1.2.9	Heteroatom-doped graphitic Carbon Nitride.....	49
1.2.10	Carbon nanomaterials Modified Graphitic Carbon Nitride.....	59
1.3	Problem Statement .....	73
1.4	Research scope and objectives .....	75
<b>CHAPTER 2 EXPERIMENTAL .....</b>		<b>76</b>
2.1	Raw Materials .....	76
2.2	Preparation of rice husk ash (RHA) from rice husk (RH).....	77
2.2.1	Synthesis of Nano Disc Silica (NDS) .....	77
2.3	Synthesis of Graphitic Carbon Nitride (g-C <sub>3</sub> N <sub>4</sub> ).....	78
2.3.1	Synthesis of Mesoporous Carbon Nitride (MCN).....	78

2.3.2	Synthesis of Oxygen doped Mesoporous Carbon Nitride (O-MCN) .....	79
2.4	Synthesis of Carbon Dots (CDs) .....	80
2.4.1	Synthesis of Carbon Dots doped Graphitic Carbon Nitride (CDs/g-C <sub>3</sub> N <sub>4</sub> ).....	80
2.5	Characterizations .....	81
2.5.1	Fourier Transform Infrared Spectroscopy (FT-IR) .....	81
2.5.2	Powder X-ray Diffraction (XRD).....	81
2.5.3	Scanning Electron Microscopy (SEM) .....	82
2.5.4	High resolution transmission electron microscopy (HR-TEM).....	82
2.5.5	N <sub>2</sub> Adsorption-Desorption Analysis (NAD) .....	83
2.5.6	Thermogravimetric Analysis (TGA).....	83
2.5.7	Zero point of charge (pHpzc) determination.....	83
2.5.8	Diffuse Reflectance UV/Vis Spectroscopy (UV-Vis DRS).....	84
2.5.9	Photoluminescence Spectroscopy (PL).....	85
2.5.10	X-Ray Photoelectron Spectroscopy (XPS).....	85
2.6	Photocatalytic Studies .....	85
2.6.1	Photocatalysis experimental set-up .....	85
2.6.2	Preparation of bisphenol A (BPA) stock solution (100 ppm).....	88



2.6.3	Effect of Parameters on Photocatalytic Activity .....	88
2.6.3(a)	Effects of pH.....	88
2.6.3(b)	Effect of BPA concentration .....	89
2.6.3(c)	Effect of catalytic loading on the photodegradation of BPA .....	89
2.6.4	Effect of radical quenchers .....	90
2.6.5	Reusability studies.....	90
2.6.6	Degradation products analysis .....	90
<b>CHAPTER 3 CHARACTERIZATION OF NANODISC SILICA.....</b>		<b>92</b>
3.1	Introduction .....	92
3.2	Characterizations .....	92
3.2.1	Transmission Electron Microscopy (TEM).....	92
3.2.2	Scanning Electron Microscope (SEM) .....	95
3.2.3	FT-IR analysis for NDS .....	97
3.2.4	Powder X-Ray diffraction (XRD) analysis .....	99
3.2.5	N <sub>2</sub> adsorption-desorption analysis .....	100
3.2.6	Thermogravimetric Analysis.....	102
3.3	Summary .....	103

<b>CHAPTER 4</b>	<b>RESULTS AND DISCUSSION.....</b>	<b>104</b>
	<b>CHARACTERIZATIONS AND PHOTOCATALYTIC ACTIVITIES OF NANODISC SILICA TEMPLATED OXYGEN DOPED MESOPOROUS CARBON NITRIDE (O-MCN).....</b>	<b>104</b>
4.1	Introduction .....	104
4.2	Optimization of O-MCN photocatalysts .....	104
4.2.1	FT-IR Analysis - Optimization of Temperature .....	104
4.2.2	The influence of glucose on the physical appearance of O-MCN nanocomposites .....	108
4.2.3	FT-IR Analysis.....	109
4.3	Powder X-Ray diffraction (XRD) analysis .....	113
4.4	Scanning Electron Microscope (SEM).....	116
4.5	Transmission Electron Microscopy (TEM).....	120
4.6	N <sub>2</sub> adsorption-desorption analysis.....	122
4.7	Point of Zero Charge (PZC) .....	127
4.8	The Ultraviolet-Visible Diffuse Reflectance Spectra (UV-vis DRS) .....	130
4.9	Photoluminescence Spectroscopy (PL).....	135
4.10	X-ray photoelectron spectroscopy (XPS)analysis.....	137

4.11	Photocatalytic activity and kinetic studies of oxygen doped mesoporous carbon nitride (O-MCN).....	153
4.11.1	Effect of initial pH on the photodegradation of BPA .....	153
4.11.2	Effect of oxygen concentration on the photodegradation of BPA.....	159
4.11.3	Effect of initial concentration of BPA on the photodegradation of BPA.....	162
4.11.4	Effect of catalyst dosages on the photodegradation of BPA.....	166
4.11.5	Effect of photolysis, P25, g-C <sub>3</sub> N <sub>4</sub> , MCN and 0.2O-MCN nanocomposite on the photodegradation of BPA .....	170
4.11.6	Scavenging Test .....	173
4.11.7	Mineralization studies .....	177
4.11.8	Proposed photo-degradation mechanism.....	178
4.11.9	Reusability .....	183
4.12	Liquid chromatography/time-of-flight/mass spectrometry (LC/TOF/MS)..	185
4.13	Summary .....	194
<b>CHAPTER 5 RESULTS AND DISCUSSION.....</b>		<b>196</b>
<b>CHARACTERIZATIONS OF CARBON DOTS MODIFIED GRAPHITIC CARBON NITRIDE NANOCOMPOSITES AND THEIR PHOTOCATALYTIC ACTIVITIES.....</b>		<b>196</b>

5.1	Introduction .....	196
5.2	Characterizations of pure g-C <sub>3</sub> N <sub>4</sub> and CDs/g-C <sub>3</sub> N <sub>4</sub> photocatalysts.....	196
5.2.1	FT-IR analysis of CDs and CDs /g-C <sub>3</sub> N <sub>4</sub> .....	197
5.2.2	Powder X-Ray diffraction (XRD) analysis .....	199
5.2.3	Scanning Electron Microscope (SEM) .....	201
5.2.4	Transmission Electron Microscopy (TEM).....	203
5.2.5	N <sub>2</sub> adsorption-desorption analysis .....	205
5.2.6	Point of Zero Charge (PZC) .....	210
5.2.7	Optical Properties .....	211
5.2.7(a)	UV-vis absorption spectrum of CDs.....	211
5.2.7(b)	The Ultraviolet-Visible Diffuse Reflectance Spectra (UV-vis DRS).....	212
5.2.8	Photoluminescence Spectroscopy (PL).....	216
5.2.8(a)	Fluorescence Quantum Yield of Carbon Dots (QY) ...	216
5.2.8(b)	Photoluminescence Spectroscopy of CDs/g-C <sub>3</sub> N <sub>4</sub> (PL)..	217
5.2.9	X-ray photoelectron spectroscopy (XPS) analysis .....	219
5.3	Photocatalytic activity and kinetic studies of carbon dots modified graphitic carbon nitride (CDs/g-C <sub>3</sub> N <sub>4</sub> ) .....	228

5.3.1	Effect of initial pH value on the photodegradation of BPA.....	229
5.3.2	Effect of initial concentration of BPA on the photodegradation of BPA.....	234
5.3.3	Effect of Carbon Dots loading on g-C <sub>3</sub> N <sub>4</sub> on the photodegradation of BPA.....	237
5.3.4	Effect of photocatalyst dosages on the photodegradation of BPA .....	240
5.3.5	Effect of P25, g-C <sub>3</sub> N <sub>4</sub> and CDs/g-C <sub>3</sub> N <sub>4</sub> on the photodegradation of BPA.....	243
5.3.6	Scavenging Test .....	246
5.3.7	Mineralization studies .....	249
5.3.8	Proposed photodegradation mechanism .....	251
5.3.9	Reusability .....	255
5.4	Liquid chromatography/time-of-flight/mass spectrometry (LC/TOF/MS)..	257
5.5	Summary .....	265
<b>CHAPTER 6 CONCLUSION AND FUTURE RECOMMENDATIONS .</b>		<b>268</b>
6.1	Conclusion.....	268
6.2	Future Recommendation .....	270

**REFERENCES .....273**

**LIST OF PUBLICATIONS**

## LIST OF TABLES

	<b>Page</b>
Table 1.1	Toxicity of BPA on aquatic species..... 20
Table 1.2	Various modification of g-C <sub>3</sub> N <sub>4</sub> -based photocatalysts reported in recent years ..... 36
Table 1.3	The summary of some of the MCNs prepared from hard templating approaches using different precursors and templates ..... 47
Table 1.4	List of oxygen doped g-C <sub>3</sub> N <sub>4</sub> photocatalysts synthesized from different precursors and routes ..... 54
Table 1.5	Lists of photocatalytic degradation of BPA using oxygen doped g-C <sub>3</sub> N <sub>4</sub> photocatalysts..... 58
Table 1.6	Lists of various CQDs synthesized using different precursors and reaction conditions ..... 64
Table 1.7	Lists of various CQDs modified g-C <sub>3</sub> N <sub>4</sub> -based photocatalysts and their photocatalytic efficiencies..... 69
Table 2.1	The list of chemicals used in this study ..... 76
Table 3.1	FTIR functional groups of NDS..... 98
Table 4.1	The XRD crystallographic parameters obtained for all the synthesized samples ..... 116
Table 4.2	The textural properties of the synthesized NDS, g-C <sub>3</sub> N <sub>4</sub> , MCN and O-MCN nanocomposites obtained from the N <sub>2</sub> adsorption-desorption analysis..... 125
Table 4.3	The absorbance and band gap of the synthesized catalysts. .... 135
Table 4.4	The elemental compositions of all the as synthesized photocatalysts obtained from XPS analysis. .... 138
Table 4.5	The XPS narrow scans showing the C 1s deconvoluted peaks of all the samples..... 151

Table 4.6	The XPS narrow scans showing the N 1s deconvoluted peaks of all the samples.....	152
Table 4.7	The XPS narrow scans showing the O 1s deconvoluted peaks of all the samples.....	152
Table 4.8	Rate constants (k) and correlation coefficients ( $R^2$ ) of pseudo-first order and second order kinetic models for BPA degradation by the 0.2O-MCN nanocomposite photocatalysts in different pH media.....	158
Table 4.9	Rate constants (k) and correlation coefficients ( $R^2$ ) of pseudo-first order kinetic models for BPA degradation by the O-MCN nanocomposite photocatalysts.....	161
Table 4.10	The pseudo first-order rate constant (k) and regression coefficient ( $R^2$ ) for the degradation of BPA under different initial concentrations of BPA solution.....	166
Table 4.11	The pseudo first-order rate constant (k) and regression coefficient ( $R^2$ ) for the degradation of BPA at different catalyst dosage.....	169
Table 4.12	The pseudo first-order rate constant and regression coefficient ( $R^2$ ) for photodegradation of BPA using different synthesized photocatalysts against P25 .....	173
Table 4.13	The rate constants and correlation coefficient values of pseudo-first order kinetics for effect of active species scavengers on the photodegradation of BPA using 0.2O-MCN.....	176
Table 4.14	Main BPA intermediates identified during photodegradation of BPA using 0.2O-MCN as determined by LC/TOF/MS .....	192
Table 4.15	Comparison of recently reported studies on oxygen doped mesoporous carbon nitride with the present study .....	195
Table 5.1	The XRD crystallographic parameters obtained for all the synthesized samples .....	201



Table 5.2	The textural properties of the synthesized pure g-C <sub>3</sub> N <sub>4</sub> and CDs/g-C <sub>3</sub> N <sub>4</sub> nanocomposites obtained from the N <sub>2</sub> adsorption-desorption analysis .....	208
Table 5.3	The absorbance and band gap of the synthesized catalysts.....	215
Table 5.4	The elemental compositions of all the as synthesized photocatalysts obtained from XPS analysis .....	220
Table 5.5	The XPS narrow scans showing the C 1s deconvoluted peaks of all the samples.....	227
Table 5.6	The XPS narrow scans showing the N 1s deconvoluted peaks of all the samples .....	227
Table 5.7	The XPS narrow scans showing the O 1s deconvoluted peaks of all the samples .....	228
Table 5.8	Rate constants (k) and correlation coefficients (R <sup>2</sup> ) of pseudo-first order and second order kinetic models for BPA degradation by 1.5CDs/g-C <sub>3</sub> N <sub>4</sub> nanocomposite photocatalysts in different pH media.....	234
Table 5.9	The pseudo first-order rate constant (k) and regression coefficient (R <sup>2</sup> ) for the degradation of BPA under different initial concentrations of BPA solution using 1.5CDs/g-C <sub>3</sub> N <sub>4</sub> .....	237
Table 5.10	Rate constants (k) and correlation coefficients (R <sup>2</sup> ) of pseudo-first order kinetic model for BPA degradation by the CDs/g-C <sub>3</sub> N <sub>4</sub> nanocomposite photocatalysts.....	240
Table 5.11	The pseudo first-order rate constant (k) and regression coefficient (R <sup>2</sup> ) for the degradation of BPA at different catalyst dosage.....	243
Table 5.12	Effect of various catalyst on BPA on the degradation of BPA ([BPA] = 20 mg L <sup>-1</sup> ; catalyst = 30 mg L <sup>-1</sup> ; pH= 10).....	246
Table 5.13	The rate constants and correlation coefficient values of pseudo-first-order kinetics for effect of active species scavengers on the photodegradation of BPA using 1.5CDs/g-C <sub>3</sub> N <sub>4</sub> .....	249

Table 5.14	Main BPA intermediates identified during photodegradation of BPA using 1.5CDs/g-C <sub>3</sub> N <sub>4</sub> nanocomposite as determined by LC/TOF/MS.....	263
Table 5.15	Comparison of recently reported studies on CDs modified graphitic carbon nitride with the present study .....	267

## LIST OF FIGURES

	<b>Page</b>
Figure 1.1	Schematic representation of photocatalysis mechanism..... 3
Figure 1.2	Structure of Bisphenol A..... 13
Figure 1.3	Schematic diagram of an adverse effect of BPA ..... 18
Figure 1.4	Process involved in a semiconductor photocatalysis..... 28
Figure 1.5	Structure of (a) triazine ring and (b) tri-s-triazine ring (Murugesan, Moses, & Anandharamakrishnan, 2019)..... 33
Figure 1.6	Thermal polymerization route to graphitic carbon nitride (Q. Su et al., 2014; Yu Zheng et al., 2017)..... 39
Figure 1.7	Schematic diagram of the hard templating method ..... 44
Figure 1.8	Structure of (a) SBA-15, (b) MCM-41 and (c) KIT-6 (Aslam et al., 2016; Chaudhary & Sharma, 2017; Raji & Pakizeh, 2013)..... 45
Figure 1.9	Band gap positioning of pure g-C <sub>3</sub> N <sub>4</sub> and different doped g-C <sub>3</sub> N <sub>4</sub> (Hasija, Raizada, Sudhaik, Sharma, Kumar, Singh, Jonnalagadda, & Kumar, 2019) ..... 50
Figure 2.1	Photocatalytic set-up and light source for the degradation of BPA..... 87
Figure 3.1	(a) TEM image and (b) particle size distribution of NDS ..... 93
Figure 3.2	(a) SEM image and (b) EDX spectrum of NDS..... 96
Figure 3.3	FT-IR spectrum of NDS..... 98
Figure 3.4	XRD spectrum of NDS..... 99
Figure 3.5	The N <sub>2</sub> adsorption-desorption isotherms (a) and porogram (b) of the synthesized NDS ..... 101
Figure 3.6	The pore size distribution using NLDFT model for NDS ..... 102
Figure 3.7	Thermogravimetric analysis (TGA) of ND ..... 103

Figure 4.1	FT-IR spectra of (a) g-C <sub>3</sub> N <sub>4</sub> and MCN and (b) optimization of O-MCN nanocomposites .....	107
Figure 4.2	The photographs of the as-synthesized pure g-C <sub>3</sub> N <sub>4</sub> , MCN and O-MCN nanocomposites polymerized at 550 °C for 1 h.....	109
Figure 4.3	FT-IR spectra of (a) NDS and (b) pure g-C <sub>3</sub> N <sub>4</sub> , MCN, 0.1O-MCN, 0.2O-MCN, 0.3O-MCN, 0.4O-MCN and 0.5O-MCN nanocomposites .....	112
Figure 4.4	XRD patterns of pure g-C <sub>3</sub> N <sub>4</sub> , MCN, 0.1O-MCN, 0.2O-MCN, 0.3O-MCN, 0.4O-MCN and 0.5O-MCN nanocomposites .....	115
Figure 4.5	The SEM images of (a) pure g-C <sub>3</sub> N <sub>4</sub> , (b) MCN, (c) 0.1 O-MCN, (d) 0.2O-MCN, (e) 0.3 O-MCN, (f) 0.4 O-MCN and (g) 0.5 O-MCN nanocomposites .....	119
Figure 4.6	The TEM images of (a) pure g-C <sub>3</sub> N <sub>4</sub> , (b) MCN, (c) 0.1O-MCN, (d) 0.2O-MCN, (e) 0.3O-MCN (f) 0.4 O-MCN and (g) 0.5O-MCN nanocomposites .....	121
Figure 4.7	The N <sub>2</sub> adsorption-desorption isotherms (inset: pore size distribution) of (a) pure g-C <sub>3</sub> N <sub>4</sub> , (b)MCN, (c) 0.1O-MCN, (d) 0.2O-MCN, (e) 0.3O-MCN, (f) 0.4O-MCN and (g) 0.5O-MCN nanocomposites .....	124
Figure 4.8	The pore size distribution using NLDFT model for (a) pure g-C <sub>3</sub> N <sub>4</sub> , (b)MCN, (c) 0.1O-MCN, (d) 0.2O-MCN, (e) 0.3O-MCN, (f) 0.4O-MCN and (g) 0.5O-MCN.....	126
Figure 4.9	The PZC plots and values of (a) pure g-C <sub>3</sub> N <sub>4</sub> , (b) MCN, (c) 0.1O-MCN, (d) 0.2OMCN, (e) 0.3O-MCN, (f) 0.4O-MCN and (g) 0.5O-MCN nanocomposites .....	129
Figure 4.10	The absorbance of pure g-C <sub>3</sub> N <sub>4</sub> , MCN and O-MCN nanocomposites .....	132
Figure 4.11	The Kubelka-Munk function of band gap calculations of (a) pure g-C <sub>3</sub> N <sub>4</sub> , (b) MCN, (c) 0.1O-MCN, (d) 0.2O-MCN, (e) 0.3O-MCN, (d) 0.4O-MCN and (g) 0.5O-MCN.....	134

Figure 4.12	Photoluminescence (PL) spectra of pure g-C <sub>3</sub> N <sub>4</sub> , MCN and O-MCN nanocomposites ranging from 300 to 700 nm.....	137
Figure 4.13	The XPS survey scans showing the C, N and O spectra for pure g-C <sub>3</sub> N <sub>4</sub> , MCN and O-MCN nanocomposites .....	138
Figure 4.14	The XPS narrow scans were showing the C 1s, N 1s and O 1s spectra of pure g-C <sub>3</sub> N <sub>4</sub> .....	140
Figure 4.15	The XPS narrow scans showing the C 1s and N 1s spectra of MCN.....	141
Figure 4.16	The XPS narrow scans showing the C 1s, N 1s and O 1s spectra of 0.1O-MCN .....	143
Figure 4.17	The XPS narrow scans showing the C 1s, N 1s and O 1s spectra of 0.2O-MCN .....	145
Figure 4.18	The XPS narrow scans showing the C 1s, N 1s and O 1s spectra of 0.3O-MCN .....	147
Figure 4.19	The XPS narrow scans showing the C 1s, N 1s and O 1s spectra of 0.4O-MCN .....	148
Figure 4.20	The XPS narrow scans showing the C 1s, N 1s and O 1s spectra of 0.5O-MCN .....	150
Figure 4.21	Effect of initial pH of BPA on the removal of BPA [BPA] = 20 mg L <sup>-1</sup> ; [0.2 O-MCN] = 50 mg L <sup>-1</sup> ; pH= 3, 5, 7, 9, 10 and 11) .	156
Figure 4.22	The plot of (a) pseudo-first order and (b) pseudo-second order kinetics of BPA photodegradation by 0.2O-MCN nanocomposite in different pH media .....	158
Figure 4.23	O-MCN nanocomposites for the degradation of BPA ([BPA] = 20 mg L <sup>-1</sup> ; [Catalyst]= 50 mg L <sup>-1</sup> ; pH = 10) .....	160
Figure 4.24	The plot of pseudo-first order kinetics of BPA photodegradation by O-MCN nanocomposites at pH 10.....	161
Figure 4.25	Effect of initial concentration of BPA on the degradation of BPA ([BPA] = 5, 10, 20, 30 40 and 50 mg L <sup>-1</sup> ; [0.2O-MCN] = 50 mg L <sup>-1</sup> ; pH = 10).....	164

Figure 4.26	The plot of pseudo-first order kinetics of BPA photodegradation by 0.2O-MCN nanocomposite under different initial concentration of BPA solution.....	165
Figure 4.27	Effect of catalyst dosage on BPA on the degradation of BPA ([BPA] = 10 mg L <sup>-1</sup> ; [0.2O-MCN] = 30, 40, 50, 60 and 70 mg L <sup>-1</sup> ; pH= 10 .....	168
Figure 4.28	The plot of pseudo-first order kinetics of BPA photodegradation using different dosages of 0.2O-MCN nanocomposite.....	169
Figure 4.29	Effect of different synthesized photocatalyst against P25 on degradation of BPA ([BPA] = 10 mg L <sup>-1</sup> ; [catalyst] = 40 mg L <sup>-1</sup> ; pH= 10) .....	171
Figure 4.30	The plot of pseudo-first order kinetics of BPA photodegradation using different synthesized photocatalysts against P25 .....	172
Figure 4.31	The Effect of active species scavengers on the photodegradation efficiency of BPA using 0.2O-MCN ([BPA] = 10 mg L <sup>-1</sup> , catalyst dosage = 40 mg L <sup>-1</sup> , pH =10).....	175
Figure 4.32	The plot of pseudo-first order kinetics of BPA photodegradation using different active scavengers .....	176
Figure 4.33	The TOC result of 0.2O-MCN on the photodegradation of BPA under visible irradiation at various time interval .....	178
Figure 4.34	VB-XPS spectra of g-C <sub>3</sub> N <sub>4</sub> and 0.2O-MCN nanocomposite.....	181
Figure 4.35	A schematic illustration of the proposed mechanism for the photodegradation of BPA using 0.2O-MCN nanocomposite .....	183
Figure 4.36	The reusability studies of 0.2O-MCN on the photodegradation efficiency of BPA ([BPA] = 10 mg L <sup>-1</sup> , catalyst dosage = 40 mg L <sup>-1</sup> , pH = 10) .....	184
Figure 4.37	The mass spectra of degradation of BPA and its intermediates in the presence of 0.2O-MCN nanocomposite .....	191
Figure 5.1	The photographs of the as-synthesized pure g-C <sub>3</sub> N <sub>4</sub> and CDs/g-C <sub>3</sub> N <sub>4</sub> nanocomposites .....	197

Figure 5.2	FT-IR spectra of pure g-C <sub>3</sub> N <sub>4</sub> , 0.5CDs/g-C <sub>3</sub> N <sub>4</sub> , 1.0CDs/g-C <sub>3</sub> N <sub>4</sub> , 1.5CDs/g-C <sub>3</sub> N <sub>4</sub> and pure CDs .....	199
Figure 5.3	XRD patterns of (a) CDs and (b) pure g-C <sub>3</sub> N <sub>4</sub> , 0.5CDs/g-C <sub>3</sub> N <sub>4</sub> and 1.0CDs/g-C <sub>3</sub> N <sub>4</sub> , 1.5CDs/g-C <sub>3</sub> N <sub>4</sub> .....	201
Figure 5.4	The SEM images of (a) pure g-C <sub>3</sub> N <sub>4</sub> , (b) 0.5CDs/g-C <sub>3</sub> N <sub>4</sub> , (c) 1.0CDs/g-C <sub>3</sub> N <sub>4</sub> and (d) 1.5CDs/g-C <sub>3</sub> N <sub>4</sub> .....	203
Figure 5.5	The HR-TEM images and particle size histograms of (a,b) CDs, (c) pure g-C <sub>3</sub> N <sub>4</sub> , (d) 0.5CDs/g-C <sub>3</sub> N <sub>4</sub> , (e) 1.0CDs/g-C <sub>3</sub> N <sub>4</sub> and (f) 1.5CDs/g-C <sub>3</sub> N <sub>4</sub> . The CDs are shown using yellow spots .....	205
Figure 5.6	The N <sub>2</sub> adsorption-desorption isotherms (inset: pore size distribution) of (a) pure g-C <sub>3</sub> N <sub>4</sub> , (b) 0.5CDs/g-C <sub>3</sub> N <sub>4</sub> , (c) 1.0CDs/g-C <sub>3</sub> N <sub>4</sub> and (d) 1.5CDs/g-C <sub>3</sub> N <sub>4</sub> nanocomposites .....	208
Figure 5.7	The pore size distribution using NLDFT model for (a) pure g-C <sub>3</sub> N <sub>4</sub> , (b) 0.5CDs/g-C <sub>3</sub> N <sub>4</sub> , (c) 1.0CDs/g-C <sub>3</sub> N <sub>4</sub> and (d) 1.5CDs/g-C <sub>3</sub> N <sub>4</sub> nanocomposites.....	210
Figure 5.8	The PZC plots and values of (a) pure g-C <sub>3</sub> N <sub>4</sub> , (b) 0.5CDs/ g-C <sub>3</sub> N <sub>4</sub> , (c) 1.0CDs/ g-C <sub>3</sub> N <sub>4</sub> and (d) 1.5CDs/ g-C <sub>3</sub> N <sub>4</sub> nanocomposites .....	211
Figure 5.9	The UV-vis absorption spectrum of CDs solution. Inset shows the fluorescence of CDs solutions under daylight (Left) and UV light (Right) .....	212
Figure 5.10	The absorbance of pure g-C <sub>3</sub> N <sub>4</sub> , 0.5CDs/g-C <sub>3</sub> N <sub>4</sub> , 1.0CDs/g-C <sub>3</sub> N <sub>4</sub> and 1.5CDs/g-C <sub>3</sub> N <sub>4</sub> nanocomposites .....	214
Figure 5.11	The Kubelka-Munk function of band gap calculations of (a) pure g-C <sub>3</sub> N <sub>4</sub> , (b) 0.5CDs/g-C <sub>3</sub> N <sub>4</sub> , (c) 1.0CDs/g-C <sub>3</sub> N <sub>4</sub> and (d) 1.5CDs/g-C <sub>3</sub> N <sub>4</sub> nanocomposites .....	215
Figure 5.12	Plot of integrated fluorescence intensity versus the corresponding absorbance for quinine sulphate (QS) and carbon dots (CDs).....	217
Figure 5.13	Photoluminescence (PL) spectra of pure g-C <sub>3</sub> N <sub>4</sub> and CDs/g-C <sub>3</sub> N <sub>4</sub> nanocomposites ranging from 300 to 700 nm.....	219

Figure 5.14	The XPS survey scans showing the C, N and O spectra for pure g-C <sub>3</sub> N <sub>4</sub> and CDs/g-C <sub>3</sub> N <sub>4</sub> nanocomposites.....	220
Figure 5.15	The XPS narrow scans showing the C 1s, N 1s and O 1s spectra of pure g-C <sub>3</sub> N <sub>4</sub> .....	221
Figure 5.16	The XPS narrow scans showing the C 1s, N 1s and O 1s spectra of 0.5CDs/C <sub>3</sub> N <sub>4</sub> nanocomposite.....	223
Figure 5.17	The XPS narrow scans showing the C 1s, N 1s and O 1s spectra of 1.0CDs/C <sub>3</sub> N <sub>4</sub> nanocomposite.....	224
Figure 5.18	The XPS narrow scans showing the C 1s, N 1s and O 1s spectra of 1.5CDs/C <sub>3</sub> N <sub>4</sub> nanocomposite.....	226
Figure 5.19	Effect of different pH of BPA on the degradation of BPA ([BPA] = 10 mg L <sup>-1</sup> ; [1.5CDs/g-C <sub>3</sub> N <sub>4</sub> ] = 30 mg L <sup>-1</sup> ; pH= 3, 5, 7, 9, 10 and 11) .....	231
Figure 5.20	The plot of (a) pseudo-first order and (b) pseudo-second order kinetics of BPA photodegradation by 1.5CDs/g-C <sub>3</sub> N <sub>4</sub> nanocomposite in different pH media .....	233
Figure 5.21	The effect of initial concentration of BPA on the degradation of BPA ([BPA] = 5,10, 20 and 30 mg L <sup>-1</sup> ; [catalyst] = 30 mg L <sup>-1</sup> ; pH = 10).....	235
Figure 5.22	The plot of pseudo-first order kinetics of BPA photodegradation by 1.5CDs/g-C <sub>3</sub> N <sub>4</sub> nanocomposite under different initial concentration of BPA solution .....	236
Figure 5.23	Effect of CDs loading on the photodegradation of BPA ([BPA] = 20 mg L <sup>-1</sup> ; [CDs/g-C <sub>3</sub> N <sub>4</sub> nanocomposites] = 30 mg L <sup>-1</sup> ; pH= 10)...	239
Figure 5.24	The plot of pseudo-first order kinetics of BPA photodegradation by CDs/g-C <sub>3</sub> N <sub>4</sub> nanocomposites at pH 10 .....	240
Figure 5.25	Effect of catalyst dosage on BPA on the degradation of BPA ([BPA] = 20 mg L <sup>-1</sup> ; [1.5CDs/g-C <sub>3</sub> N <sub>4</sub> ] = 20, 30 and 40 mg L <sup>-1</sup> ; pH= 10).....	242



Figure 5.26	The plot of pseudo-first order kinetics of BPA photodegradation using different dosages of 1.5CDs/g-C <sub>3</sub> N <sub>4</sub> nanocomposite.....	243
Figure 5.27	Effect of various synthesized photocatalyst against P25 on degradation of BPA ([BPA] = 20 mg L <sup>-1</sup> ; [catalyst] = 30 mg L <sup>-1</sup> ; pH= 10) .....	244
Figure 5.28	The plot of pseudo-first order kinetics of BPA photodegradation using various synthesized photocatalysts.....	245
Figure 5.29	Effect of active species scavengers on the photodegradation efficiency of BPA using 1.5CDs/g-C <sub>3</sub> N <sub>4</sub> ([BPA] = 20 mg L <sup>-1</sup> , catalyst dosage = 30 mg L <sup>-1</sup> , pH = 10).....	247
Figure 5.30	The plot of pseudo-first order kinetics of active species scavengers on the photodegradation of BPA .....	249
Figure 5.31	The TOC result of 1.5CDs/g-C <sub>3</sub> N <sub>4</sub> on the photodegradation of BPA under visible irradiation at various time interval.....	251
Figure 5.32	VB-XPS spectra of g-C <sub>3</sub> N <sub>4</sub> and 1.5CDs/g-C <sub>3</sub> N <sub>4</sub> nanocomposite.....	252
Figure 5.33	A schematic illustration of the proposed mechanism for the photodegradation of BPA using 1.5CDs/g-C <sub>3</sub> N <sub>4</sub> nanocomposite ....	255
Figure 5.34	The reusability studies of 1.5CDs/g-C <sub>3</sub> N <sub>4</sub> on the photodegradation efficiency of BPA ([BPA] = 20 mg L <sup>-1</sup> , catalyst dosage = 30 mg L <sup>-1</sup> , pH = 10).....	256
Figure 5.35	The mass spectra of degradation of BPA and its intermediates in the presence of 1.5CDs/g-C <sub>3</sub> N <sub>4</sub> nanocomposite.....	262

## LIST OF SCHEMES

	<b>Page</b>
Scheme 3.1 Schematic illustration of formation of NDS derived from RH.....	94
Scheme 4.1 The proposed possible pathways during the photocatalytic degradation of BPA in the presence of 0.2O-MCN photocatalyst...	193
Scheme 5.1 The proposed possible pathways during the photocatalytic degradation of BPA in the presence of 1.5CDs/g-C <sub>3</sub> N <sub>4</sub> photocatalyst .....	264

## LIST OF SYMBOLS

$e^-$	Electrons
$g\text{-C}_3\text{N}_4$	Graphitic carbon nitride
$h^+$	Positive holes
HF	Hydrofluoric Acid
$\text{HNO}_3$	Nitric acid
k	Rate constant
$\text{O}_2^{\bullet-}$	Superoxide radical
$\bullet\text{OH}$	Hydroxyl radical
$\text{OH}^-$	Hydroxyl ion
$\text{TiO}_2$	Titanium oxide
ZnO	Zinc oxide

## LIST OF ABBREVIATIONS

AA	Ascorbic acid
AOP	Advanced Oxidation Processes
AR	Androgen receptor
BBB	Blood-brain barrier
BET	Brunauer, Emmett and Teller
BJH	Barett, Joyner and Halenda
BPA	Bisphenol A
$C_0$	Initial concentration
$C_t$	Final concentration
CB	Conduction band
CDs	Carbon dots
CDs	Compact discs
Clx-BPA	Chlorinated derivatives
CNTs	Carbon nanotubes
CQDs	Carbon quantum dots
DFT	Density Functional Theory
EDTA	Ethylenediaminetetraacetic acid
EDCs	Endocrine disrupting compounds
$E_g$	Band gap
EOCs	Emerging organic contaminants
EPA	Environmental Protection Agency
ER	Estrogen receptor
EU	European Union
FTIR	Fourier Transform Infrared Spectroscopy
FWHM	Full Width at Half Maximum
G	Graphene
GA	Gallic acid

HRTEM	High Resolution Transmission Electron Microscopy
IUPAC	International Union of Pure and Applied Chemistry
KBr	Potassium bromide
LC/TOF/MS	Liquid chromatography/time-of-flight/mass spectrometer
LH	Langmuir–Hinshelwood
MeOH	Methanol
MCN	Mesoporous Carbon Nitride
MW	Microwave
NAD	N <sub>2</sub> Adsorption-Desorption
NDS	Nano disc silica
NLDFT	Non-Local Density Functional Theory
O-MCN	Oxygen doped mesoporous carbon nitride
PL	Photoluminescence
POPs	Persistent organic pollutants
PPCPs	Pharmaceutical and personal care products
PTS	Persistent toxic substances
PZC	Point of zero charge
QS	Quinine sulphate
QY	Quantum yield
RH	Rice husk
RHA	Rice husk silica
ROS	Reactive oxygen species
SEM	Scanning Electron Microscopy
SDAs	Structure directing agents
TEOS	Tetraethyl orthosilicate
TGA	Thermogravimetric Analysis
THR	Thyroid hormone receptor
TOC	Total organic carbon
TWW	Treated wastewater
UV-Vis DRS	UV-Visible diffuse reflectance spectroscopy

VB	Valence band
VB-XPS	Valence band X-ray photoelectron spectroscopy
WHO	World Health Organization
XRD	Powder X-ray Diffraction

## **LIST OF APPENDICES**

Appendix A      LIST OF PUBLICATIONS

**PENINGKATAN PENGURAIAN FOTOPEMANGKINAN BISFENOL A DI  
BAWAH SINARAN CAHAYA NAMPAK MENGGUNAKAN KARBON  
NITRIDA BERLIANG MESO TERDOP OKSIGEN BERTEMPLAT NANO  
CAKERA SILIKA ABU SEKAM PADI DAN TITIK KARBON DIUBAH SUAI  
NITRIDA KARBON GRAFIT**

**ABSTRAK**

Satu siri karbon nitrida berliang meso terdop oksigen (O-MCN) dengan kandungan oksigen yang berbeza dan titik karbon diubah suai grafit karbon nitrida (CDs/g-C<sub>3</sub>N<sub>4</sub>) disintesis melalui kaedah polimerisasi termal dan kaedah polimerisasi termal dibantu gelombang mikro, masing-masing, untuk fotodegradasi bisphenol A (BPA) di bawah sinaran cahaya nampak. O-MCN dilabel sebagai *x*O-MCN (*x* = 0.1, 0.2, 0.3, 0.4, dan 0.5 g glukosa) manakala CDs/g-C<sub>3</sub>N<sub>4</sub> dilabel sebagai *y*CDs/g-C<sub>3</sub>N<sub>4</sub> (*y* = 0.5, 1.0 dan 1.5 ml CD). Spektroskopi inframerah transformasi Fourier (FTIR), difraksi sinar-X (XRD), mikroskopi elektron imbasan (SEM), mikroskopi elektron transmisi (TEM), penjerapan-penyahjerapan nitrogen (NAD), spektroskopi pantulan sinar UV/Sinar nampak (UV-vis DRS), spektroskopi fotopendarcahaya (PL), dan Spektroskopi fotoelektron sinar-X (XPS) digunakan untuk mencirikan nanokomposit. 0.2O-MCN mempunyai penyingkiran BPA tertinggi (97%) pada keadaan optimum (40 mgL<sup>-1</sup> 0.2O-MCN, 10 mgL<sup>-1</sup> BPA, pada pH 10). Kadar penyingkiran adalah 0.0132 min<sup>-1</sup>, iaitu 1.8 kali ganda daripada g-C<sub>3</sub>N<sub>4</sub> tulen. Analisis XPS mengesahkan atom oksigen menggantikan atom nitrogen dalam rangka g-C<sub>3</sub>N<sub>4</sub>. Ujian hapus sisa menunjukkan bahawa <sup>+</sup> adalah spesies yang paling aktif, diikuti oleh superoksida (O<sub>2</sub><sup>-</sup>) dan radikal hidroksil (<sup>•</sup>OH). Nanokomposit dapat



digunakan semula sehingga lima kali tanpa kehilangan ketara dalam aktiviti fotopemangkinanya. Dengan kadar fotodegradasi  $0,01014 \text{ min}^{-1}$  dan kecekapan penyingkiran 90% BPA dalam 180 minit, nanokomposit 1.5CDs/g-C<sub>3</sub>N<sub>4</sub> yang dioptimumkan menunjukkan penurunan BPA fotopemangkinan yang luar biasa. Peningkatan aktiviti fotopemangkinan 1.5CDs/g-C<sub>3</sub>N<sub>4</sub> disebabkan oleh kesan sinergistik ciri-ciri CD, yang mengakibatkan peningkatan pemisahan pembawa cas dan struktur jalur yang dapat ditala. CD disambungkan ke permukaan g-C<sub>3</sub>N<sub>4</sub> melalui pautan C-O. CD yang terikat mengurangkan struktur celah pita g-C<sub>3</sub>N<sub>4</sub>, lalu mencegah pengumpulan semula cas. Spesies aktif serupa seperti di O-MCN dikenal pasti bertanggungjawab dalam fotopenguraian BPA. Pemangkin hibrid menunjukkan kebolegunaan semula yang baik sehingga lima kitaran. Pengantara yang dikenal pasti melalui melalui kromatografi cecair / spektrometri masa / penerbangan / masa (LC/TOF/MS) digunakan untuk mendalilkan mekanisme penguraian BPA. Penyelidikan ini memberikan pemahaman yang lebih mendalam mengenai modifikasi struktur elektronik dan mekanisme seperti fotosensitisasi dalam sistem fotopemangkinan bahan berasaskan g-C<sub>3</sub>N<sub>4</sub>.

**ENHANCED PHOTOCATALYTIC DEGRADATION OF BISPHENOL A  
UNDER VISIBLE LIGHT IRRADIATION USING NANO DISC RICE HUSK  
ASH SILICA-TEMPLATED OXYGEN DOPED MESOPOROUS CARBON  
NITRIDE AND CARBON DOTS MODIFIED GRAPHITIC CARBON  
NITRIDE**

**ABSTRACT**

A series of oxygen doped mesoporous carbon nitride (O-MCN) was synthesized via thermal polymerization method. Another series of carbon dots modified graphitic carbon nitride (CDs/g-C<sub>3</sub>N<sub>4</sub>) was also synthesized via microwave assisted thermal polymerization method. Both were used for the photodegradation of bisphenol A (BPA) under visible light irradiation. The O-MCN were labelled as *x*O-MCN (*x* = 0.1, 0.2, 0.3, 0.4 and 0.5 g glucose) whereas the CDs/g-C<sub>3</sub>N<sub>4</sub> were labelled as *y*CDs/g-C<sub>3</sub>N<sub>4</sub> (*y* = 0.5, 1.0 and 1.5 ml CDs). The Fourier transform infrared (FTIR) spectroscopy, X-ray diffraction (XRD) analysis, scanning electron microscopy (SEM), transmission electron microscopy (TEM), nitrogen adsorption-desorption (NAD), UV-vis diffuse reflectance spectroscopy (UV-vis DRS), photoluminescence (PL) spectroscopy, and X-ray photoelectron (XPS) spectroscopy were used to characterize the nanocomposites. The 0.2O-MCN have the highest removal of BPA (97%) under optimum conditions (40 mgL<sup>-1</sup> 0.2O-MCN, 10 mgL<sup>-1</sup> BPA, at pH 10). The removal rate was 0.0132 min<sup>-1</sup>, which is 1.8 times that of pure g-C<sub>3</sub>N<sub>4</sub>. The XPS analysis confirms that the oxygen atoms substituted the nitrogen atom in the framework of g-C<sub>3</sub>N<sub>4</sub>. The scavenging experiments revealed that h<sup>+</sup> are the most active species, followed by superoxide (O<sub>2</sub><sup>•-</sup>) and hydroxyl radicals (•OH).

The nanocomposite was able to be reused up to five times without significant loss in its photocatalytic activity. With a photodegradation rate of  $0.01014 \text{ min}^{-1}$  and 90% BPA removal efficiency in 180 minutes, the optimized 1.5CDs/g-C<sub>3</sub>N<sub>4</sub> nanocomposite demonstrated outstanding photocatalytic BPA degradation. The enhanced photocatalytic activity of 1.5CDs/g-C<sub>3</sub>N<sub>4</sub> is due to the synergistic effects of CD characteristics, which resulted in increased charge carrier separation and tunable band structure. The CDs are anchored to the g-C<sub>3</sub>N<sub>4</sub> surface via a C–O link. The bonded CDs reduced the bandgap structure of g-C<sub>3</sub>N<sub>4</sub>, preventing charge recombination. Similar active species as in O-MCN were identified to be responsible in photodegrading the BPA. The photocatalysts show good reusability after five cycles. The identified intermediates by Liquid chromatography/time-of-flight/mass spectrometry (LC/TOF/MS) were used to postulate the mechanisms for BPA breakdown. This research provides a deeper understanding of the electronic structure modification and photosensitization-like mechanism in the photocatalysis system of g-C<sub>3</sub>N<sub>4</sub>-based materials.

## **CHAPTER 1 INTRODUCTION AND LITERATURE REVIEW**

### **1.1 Background**

Even though water covers about 70% of the earth surface, unfortunately, a significant part of it has been exposed to pollution due to organic evolution and human activities (Beniah Obinna & Ebere, 2019). The emerging organic contaminants (EOCs) are heterogeneous groups of substances that consist of several chemical classes. They are mainly produced or generated from anthropogenic compounds (harmful chemical released into the environment due to human activities). The EOCs have been confirmed to have detrimental effects on life, continuance and progenitive success on living organisms. Some EOCs demonstrate or show disrupting endocrine effects, which changes the hormonal equilibrium of living organisms. These particular groups of famous compound (EOC) are considered to be endocrine-disrupting compounds (EDCs) (Joanna Karpinska and Urszula Kotowska, 2019). One of the frequently detected EDCs in the aquatic environment is bisphenol A (BPA). Bisphenol A (BPA) is a common EDC found in the aquatic environment. BPA is a chemical compound that is commonly used in manufacturing of flame retardants, polycarbonate plastics, and epoxy resins (Frankowski, Zgoła-Grześkowiak, Smulek, & Grześkowiak, 2020). Most water treatment technologies could not remove the total dosage of BPA in water; hence, there is a continuous high risk to humans and other living organisms to this compound (Tursi, Chatzisyneon, Chidichimo, Beneduci, & Giuseppe Chidichimo, 2018).

The treatment of water using conventional techniques such as flocculation, chlorination, precipitation, sedimentation, and filtration usually remove cyanobacteria and low levels of (cyano) contaminant (Serrà, Philippe, Perreault, & Garcia-Segura, 2021) but are unable to remove the EDCs effectively; thus, via the effluent discharges, the EDCs escape intact into the aquatic system (Davididou, Nelson, Monteagudo, Durán, Expósito, & Chatzisyneon, 2018). The cost of operation of the techniques is very high and can produce secondary contaminants that further instigate a more toxic environment. Chlorination, for example, is a chemical procedure that removes organic molecules from water. Chlorine, the most commonly used disinfectant and oxidant for water treatment, results in the development of potentially harmful by-products of disinfection, for example, chlorate, chlorite, halomethane species, and haloacetamides (Rojas & Horcajada, 2020). The high reactivity of BPA with disinfectant hypochlorite and free chlorine radicals results in the development of its more commonly observed chlorinated derivatives (Clx-BPA) and at higher concentrations than BPA in tap water (Martín, Santos, Malvar, Aparicio, & Alonso, 2020). In addition, Clx-BPA is more active in both artificial environment and living organism studies than BPA. It results in several chlorinated intermediate residual concentrations with endocrine and other detrimental biological properties (Frankowski et al., 2020).

Photocatalysis has come to light as a captivating approach for the removal of organic contaminants, including EDCs, due to its ability to completely mineralize the pollutants (Chiu, Chang, Chen, Sone, & Hsu, 2019; X. Gao, Kang, Xiong, & Chen, 2020). Photocatalytic water treatment for environmental remediation is a promising Advanced Oxidation Processes (AOP). Photocatalysis efficiently mineralises various troublesome organics by creating active species ( $O_2^{\bullet -}$ ,  $\bullet OH$  and  $h^+$ ) (Lin, Jiang, Chen,

Xu, & Wang, 2020). Photocatalysis occurs when a semiconducting material is exposed to light, thereby forming electron and hole pair (Ameta, Solanki, Benjamin, & Ameta, 2018). Figure 1.1 shows the formation of charge carriers, by exposing a semiconductor to light with the same amount of energy or higher than the band gap of the photocatalyst. The electrons ( $e^-$ ) separates from the hole and migrates to the conduction band while holes ( $h^+$ ) remain in the valence band. Molecules that are adsorbed on the photocatalyst surface materials are reduced and oxidised as a result (Rueda-Marquez, Levchuk, Fernández Ibañez, & Sillanpää, 2020). Hence, fashioning out a design to create or modify a photocatalyst to produce the active radicals is very significant in this study (W. Deng, Zhao, Pan, Feng, Jung, Abdel-Wahab, Batchelor, & Li, 2017).

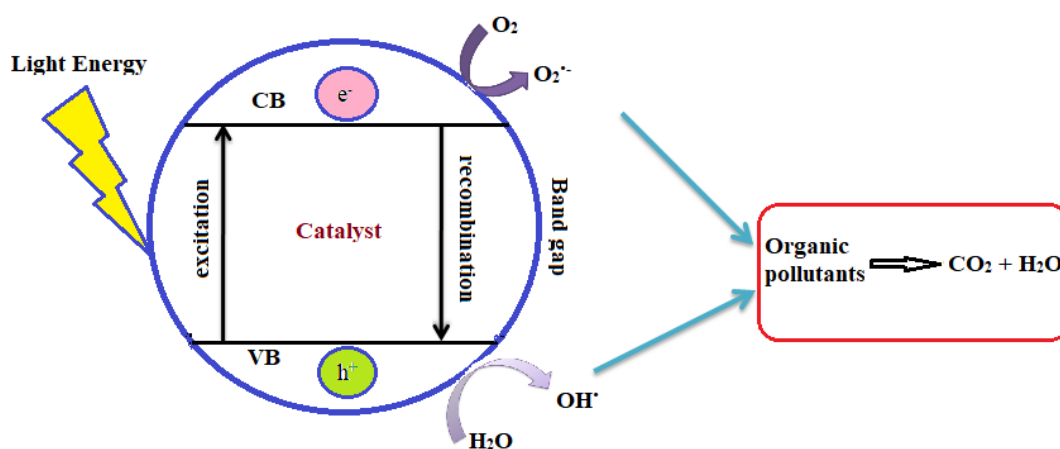


Figure 1.1 Schematic representation of photocatalysis mechanism

The primary factors that influence the photocatalytic performance of a semiconductor are broad bandgap, high surface area, carrier separation, stability and migration efficiency (Photo-oxidation, Yaqoob, Habibah, Serr, Nasir, & Ibrahim,

2020; Quesada-Cabrera & Parkin, 2020). Graphitic carbon nitride (g-C<sub>3</sub>N<sub>4</sub>) was discovered more recently and it has excellent photocatalytic oxidation technology in water treatment, necessitating researchers to develop and extend the application of g-C<sub>3</sub>N<sub>4</sub> (L. Deng, Jiang, Tang, & Li, 2018). The g-C<sub>3</sub>N<sub>4</sub> is currently being researched as a new photocatalyst made of carbon nitride for recovering the photocatalytic activity of commonly used photocatalysts like ZnO and TiO<sub>2</sub>. It demonstrated excellent photocatalytic behaviour in visible light region without using any metal co-catalyst (Darkwah & Oswald, 2019).

## **1.2 Literature Review**

### **1.2.1 Water pollution and the environment**

Water pollution is defined as water contamination with harmful materials such as industrial effluent wastes, domestic wastes, marine dumping, radioactive waste, and atmospheric deposition (S. Ahmed & Ismail, 2017). Human activities are the main contributor to water pollution. Many water supplies are polluted due to ignorance and are unsuitable for drinking and other purposes. In addition, due to the dumping of untreated contaminants, chemicals and toxic waste from thousands of factories directly into the water body, residual freshwater supplies are increasingly contaminated (Jayaswal, Sahu, & Gurjar, 2018). Severe water contamination has resulted from inadequate regulation of the release of contaminants into the water. The polluting elements in the marine ecosystem have become highly complex relative to conditions in the past, as some rising pollutants contribute to the emergence of a new challenge to water security (Bian, Xiong, & Zhu, 2018). An increase in water consumption, climate changes, and human activities on the environment is already causing a water crisis or environmental catastrophe. In

addition, the widespread use and disposal of chemicals in medicine, industry, and agriculture leads to the accumulation of organic contaminants in water (Sousa, Ribeiro, Barbosa, Pereira, & Silva, 2018).

Toxic organic compounds are mainly from the heavy use of chemical substances in day-to-day activities and unregulated drug access. As a result, there was an increase in waste production and a lot of contamination in the environment from both old and new organic substances (Joanna Karpinska and Urszula Kotowska, 2019). Several organic contaminants that are persistent have been linked to cancer and have other negative consequences in the aquatic environment (Ambauen, Muff, Mai, Hallé, Trinh, & Meyn, 2019). Heavy metals called inorganic compounds enter the marine environment through air deposition, deterioration of the geological matrix, or anthropogenic activities such as industrial waste, residential sewage, and waste produced by mining (S. Thangamalathi & Anuradha, 2018). In general, heavy metals enter the marine environment by atmospheric accumulation, geological matrix degradation or because of anthropogenic activities caused by industrial waste, domestic sewage and mining waste (Kurwadkar, 2019; S. Thangamalathi & Anuradha, 2018).

Amongst these contaminants, toxic organic compounds are numbered in millions with different functional groups, properties, and applications. They are persistent in the environment because they are common industrial organic wastes like organic dyes, pesticides, personal care products, detergents and pharmaceuticals (H. Dong, Qiang, & Richardson, 2019; F. Lu & Astruc, 2020; Richardson & Ternes, 2018; Y. Yang, Ok, Kim, Kwon, & Tsang, 2017). These organic pollutants and their toxic derivatives make the water unhealthy for consumption (Mosharraf, Nazmul



Islam, & M. Rahm, 2012). Hence, there is need to know the classes of the organic compounds, their origins, and the impact they have on the environment and human health. This is to be able to control their entry and instigate strategies in treating the water from persistent organic pollutants.

### **1.2.2 Toxic organic pollutants**

Organic pollutants are chemical contaminants that contain essentially carbon covalently bonded with other compounds. They are considered poisonous or carcinogenic in nature, and large amounts of water create severe and widespread concern (Beniah Obinna & Ebere, 2019). Most organic pollutants are persistent in the environment and resistant to degradation; hence, bioaccumulation poses adverse effects on the ecosystem. This class of organic pollutants are known as persistent organic pollutants (POPs) (Verla, Enyoh, Verla, & Nwarnorh, 2019), which are constantly present in the environment due to increased industrialization and the increase in anthropogenic activities, such as wastewater discharge and incomplete petrochemical combustion (S. Das, Aria, Cheng, Souissi, Hwang, & Ko, 2020). POPs are proclivity toward bioaccumulation, with sluggish metabolism in living organisms. Hence, remain in our body for a long time and makes it highly toxic (Alharbi, Basheer, Khattab, & Ali, 2018).

The four classification of POPs are listed below (Pi, Li, Xia, Wu, Li, Xiao, & Li, 2018);

- (a) Persistent toxic substances (PTS): It refers to a class of highly harmful and resistant organic chemical contaminants that are biodegradable in the natural environment. Most PTS are aromatic compounds consisting of two or more benzene rings, usually substituted by chlorine.

- (b) Pesticides and herbicides: Almost all pesticides and herbicides are poisonous and persistently stable, significantly destroying habitats and harming human health when impregnated with water. They enter the water by runoff, leaching or spraying (Hassaan & El Nemr, 2020).
- (c) Antibiotics: Antibiotic drugs are primarily derived from human excretion, pharmaceutical and hospital sewage discharge, animal feed and aquaculture. In aquatic environments, trace levels of antibiotics can lead to antibiotic resistance and adversely affect marine wildlife, ecosystems, and human health. The widespread use of antibiotics has led to their frequent detection (Q. Li & Zhang, 2020).
- (d) Phenols: Phenols are considered toxic and carcinogenic, usually with harmful effects, even in dilute solutions. Phenolic wastewater originates mainly from the petrochemical, resin, plastics, synthetic fibre and coal industries, oil refineries. These phenolic compounds are regarded as priority contaminants because of their toxicity and persistence in the environment and feature on the US Environmental Protection Agency's list of hazardous substances (EPA) (Mainali, 2020).

There is currently growing concern about new organic synthetic compounds in the environment referred to as new or emerging organic contaminants (EOCs). Such compounds have been present in the atmosphere for a long time, but they were not detected until new and more sensitive analytical methods were developed. They are also referred to as emerging POPs (Lorenzo, Campo, & Picó, 2018).

### **1.2.2(a) Emerging Organic Contaminants (EOCs)**

The emerging organic contaminants (EOCs) are any organic chemical that is a man-made or naturally occurring with little or no environmental regulation. However, it has the ability to invade the surroundings and cause documented or suspected negative environmental consequences on human health (Stewart, M. and Tremblay, 2020). The EOCs are mostly human-derived organic chemicals that are extensively distributed in the environment and have terrible health effects (Bernot, Bernot, & Matthaei, 2019). Pharmaceuticals, personal care products, pesticides, surfactants, industrial additives and endocrine-disrupting compounds (EDCs) are among the toxins in the EOCs group, which have serious adverse effects on living organisms and the climate (EDCs) (Stewart, M. and Tremblay, 2020). Since EOCs have been detected at trace levels in different food products (Santarelli, Migliorati, Pomilio, Marfoggia, Centorame, D'Agostino, D'Aurelio, Scarpone, Battistelli, Di Simone, Aprea, & Iannetti, 2018), stringent controls have been implemented by the European Union (EU) on food products entering the European market. Seafood has earned considerable attention among food commodities due to increasing reports on trace organic EOCs in fish, mussels, clams and molluscs from various parts of the world. In seafood samples obtained from European countries' marine and coastal waters, EOCs such as phenolic EDCs, dioxins, polyaromatic hydrocarbons, and pharmaceutical compounds were detected at trace levels (Omar, Aris, Yusoff, & Mustafa, 2019; Philip, Aravind, & Aravindakumar, 2018). It is, therefore, possible to identify EOCs as either pharmaceuticals, nanomaterials, personal care products (PPCPs), or endocrine-disrupting chemicals (EDCs) (Bwapwa & Jaiyeola, 2019).

Due to rising population, increasing urbanization and climate change-induced changes in precipitation patterns (weather), many regions such as the Middle East,

East Africa, and the U.S. Southwest face unprecedented water crisis. Treated wastewater (TWW) is accepted as a reliable alternative to increasing irrigation to combat water scarcity and meet the increasing demand for water in agricultural production (Q. Fu, Malchi, Carter, Li, Gan, & Chefetz, 2019). In 2017, human-caused global warming reached an average of 1°C above pre-industrial levels, as reported by Intergovernmental Panel on Climate Change. The global mean temperature could rise by 3.5 °C by 2100, with regional average global temperature fluctuations ranging from 1.4 to 5.8 °C. Climate change is predicted to be responsible for roughly 20% of the worldwide increase in water shortage, affecting the growth and functioning of societies worldwide, both socially and economically (Ungureanu, Vlăduț, & Voicu, 2020). Approximately 5.6 billion m<sup>3</sup> of TWW is used globally for irrigation purposes per year, even though it is less than 1% of the global irrigation volume. More than 85 % of the TWW produced in Israel is used for irrigation, while about 38 % of the TWW is used for irrigation in Jordan, and about 46 % of the TWW used in California is used for agricultural land (Ben Mordechay, Tarchitzky, Chen, Shenker, & Chefetz, 2018). The EOCs found in TWW used for irrigation of agricultural products will be absorbed by the crops and eventually join the food chain when humans consume (González García, Fernández-López, Polesel, & Trapp, 2019). A rising number of studies have recorded the absorption and accumulation of pharmaceutical and personal care products (PPCPs) by plants since around 2009 (Q. Fu et al., 2019). Despite the low concentration of PPCPs generally detected, their continuous introduction from various pathways into the environment and their bioactivity and established mode of action make them concern as emerging environmental pollutants that may pose potential ecotoxicological effects in the environment (Christou, Karaolia, Hapeshi, Michael, & Fatta-Kassinou, 2017).

### **1.2.2(b) Endocrine Disrupting Compounds**

Chemicals unwittingly messing with the endocrine communication system and cause detrimental health effects are endocrine-disrupting chemicals (EDCs) (Lucaccioni, Trevisani, Marrozzini, Bertoncelli, Predieri, Lugli, Berardi, & Iughetti, 2020). EDCs are therefore defined as “chemicals that stand in the way of any aspect of the action of hormones” (Lauretta, Sansone, Sansone, Romanelli, & Appetecchia, 2019). EDCs consist of natural and synthetic compounds readily released by household, municipal, hospital, industrial and livestock waste into the environment. Not to mention, in humans, they can imitate and block the endocrine system, causing severe consequences such as cancer, irregular reproductive growth and metabolic disorders and a wide range of human well-being issues (Ismail, Wee, Haron, Kamarulzaman, & Aris, 2020). Several processes can disrupt the endocrine system, including imitating or eliminating natural hormone, synthesis, secretion, transport, metabolism, and imitating hormone activity at the receptor binding and signal transduction levels (Kassotis & Stapleton, 2019; Küblbeck, Vuorio, Niskanen, Fortino, Braeuning, Abass, Rautio, Hakkola, Honkakoski, & Levonen, 2020)

Over 460 million people have type II diabetes, and 650 million adults are obese, according to the World Health Organization (WHO), making these diseases major health issues and a huge economic burden worldwide (International Diabetes Federation, 2019). By 2045, the global burden of diabetes is expected to cross a whopping 629 million people. The WHO expects metabolic disorders to be a major cause of death by 2030, bringing tremendous economic stress on healthcare systems worldwide (Kassotis & Stapleton, 2019). Much evidence shows that EDCs play a significant part in causing cancer, diabetes, obesity, infertility, growth development problems, and metabolic syndrome (De Coster & Van Larebeke, 2012). Even though

they are detected in low concentration, they can cause damages at long-term low-dose exposure (Bao, Huang, Hu, & Yin, 2020).

Since the beginning of the Industrial Revolution in 1784, contaminants have primarily arisen from industrial origin. Water sources, such as rivers, provide a simple way to dispose of industrial waste, and groundwater is frequently contaminated by leaching from dumping sites, potentially exposing people to waterborne diseases. After the original reference in 1965, the presence of EDCs in drinking water was reintroduced as a serious concern in the mid-1970s, albeit there was little investigation after that (Wee & Aris, 2019). It is suspected that EDCs enter the aquatic environment as sewage effluent or other forms of contamination. However, little evidence on the occurrence of these compounds in drinking water is still available. Many of these EDCs are very stable and resistant to water treatment, raising concern that they can move via relatively large amounts of drinking water (Oberflächenwasser, Brueller, Inreiter, Boegl, Rubasch, Saner, Humer, Schuhmann, Hartl, Brezinka, Wildt, & Allerberger, 2018).

Two typical EDCs in the water environment have been reported (X. Gao et al., 2020):

- (i) Oestrogen: This substance is found in sewage ( $\text{ng L}^{-1}$ ) at low concentrations but has high oestrogen action, which includes natural steroidal estrogens such as  $17\beta$ -estradiol (E2) and  $17\alpha$ -ethynylestradiol synthetic contraceptive (EE2).
- (ii) Endocrine-disrupting phenolic compounds have low estrogenic activity, but have significant concentration in wastewater, which can reach micrograms per litre such as nonylphenol (NP) and bisphenol A (BPA).

Exposure to these compounds by man and animals is associated with adverse health and reproductive results; hence, the presence of these EDCs in water has become a public health problem. For example, exposure to bisphenol A (BPA) and phthalates reduces fertility in mammals by triggering primordial follicles prematurely and altering sex-steroid hormone levels (Gonsioroski, Mourikes, & Flaws, 2020). BPA is among the best-studied EDCs that may adversely affect the early development stage and one of the most widely produced chemicals in the world. Most individuals are exposed to this chemical daily by eating food and beverages from polycarbonate containers into which BPA has leached, including reusable bottles and baby bottles (Basak, Das, & Duttaroy, 2020).

### **1.2.3 Bisphenol A (BPA)**

Bisphenol A [2, 2-bis (4-hydroxyphenyl) propane] (BPA), as shown in Figure 1.2, is an organic compound that belongs to bisphenols and derivatives of diphenylmethane. It has a molecular weight of  $228.18 \text{ g mol}^{-1}$ . The BPA is a white crystalline solid at room temperature. It melts at  $156 \text{ }^\circ\text{C}$  and boils at  $220 \text{ }^\circ\text{C}$ . Its solubility in water is  $120 \text{ mg L}^{-1}$  at  $25 \text{ }^\circ\text{C}$ . A Russian chemist, Alexander P Dianin was the first to synthesize BPA in 1891 using a condensation reaction of two phenol molecules and one acetone molecule with hydrogen chloride and ion exchange resin as a catalyst (Ohore & Songhe, 2019). Since the 1940s, BPA has been widely used to manufacture plastic containers, thermal papers, can liners/coats, and DVDs. The BPA is classified as endocrine-disrupting compounds because of its estrogenic properties (Almeida, Raposo, Almeida-González, & Carrascosa, 2018; Ohore & Songhe, 2019). Dowds and Lawson, who discovered their estrogenic properties in vivo, obtained the first evidence of BPA's mechanisms of action in 1936 (Cimmino, Fiory, Perruolo, Miele, Beguinot, Formisano, & Oriente, 2020). Estrogenic

compounds have similar properties to the  $17\beta\text{E}2$  hormone, whose effects are induced by interactions with the oestrogen receptor and cell systems.  $17\beta\text{E}2$  hormone is the main natural ovarian-generated oestrogen (Pamplona-Silva, Mazzeo, Bianchi, & Marin-Morales, 2018). Therefore, even at very low concentrations, BPA can induce estrogenic effects, causing reproductive and developmental disorders in both humans and wild animals by operating and blocking the physiological activity of oestrogen receptors analogously or acting as testosterone antagonists in the cell (Cimmino et al., 2020). BPA belongs to the Endocrine Disruptive Chemicals (EDCs) group and is acutely toxic to living organisms because of its strong evidence of disruptive endocrine activity (Adeyi & Babalola, 2019).

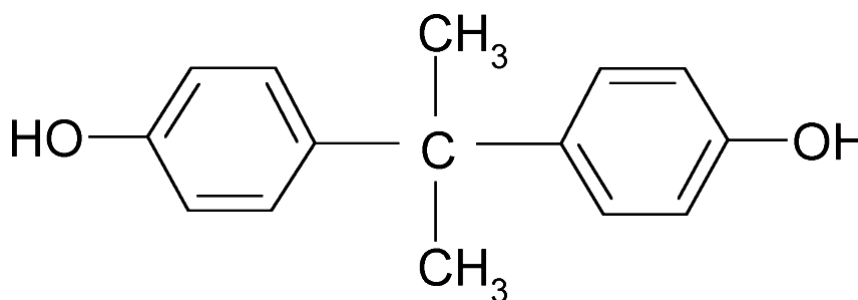


Figure 1.2 Structure of Bisphenol A

### 1.2.3(a) Sources of BPA

The BPA is one of the most rapidly and perhaps the most representative member of the emerging organic pollutants in the environment due to its excessive use (up to tens of thousands of  $\text{ng L}^{-1}$  in surface water and thousands of  $\text{ng g}^{-1}$  in sediments) (Z. Huang, Zhao, Yang, Jia, Zhang, Chen, Liu, Yang, Xie, & Ying, 2020). Around 8 million tonnes of BPA are produced and used annually, mainly in the manufacturing of epoxy resins and polycarbonate polymers (Radwan, Ibrahim,



Adel, & Farouk, 2020). Polycarbonates are hard plastics used in toys, bottles of water, glass lenses and compact discs (CDs), and epoxy resins as strong adhesives, dental sealants, and protective linings in cans (Löfroth, Ghasemimehr, Falk, & Vult von Steyern, 2019). Because they can withstand high temperatures and high-impact collisions, BPA-based polycarbonate plastics are rigid and stable. Because they have the ability to withstand heating in microwave ovens, these properties make them useful as safety equipment and food packaging materials. BPA extends the life-span of food and beverage products by being an ingredient in epoxy resins used to make protective coatings such as the insides of aluminum and metal cans (as well as the lid closures of glass jars and bottles) (Campanale, Massarelli, Savino, Locaputo, & Uricchio, 2020). The extensive use of BPA has contributed to its exposure to human and marine animals through the leaching of packaging materials into food and water, thus its declaration by regulatory authorities in several countries as a hazardous material (Alam & Deen, 2020).

The widespread occurrence of BPA in the ecosystem has been documented to include wastewater discharge, river water and sediments, given the comprehensive applications of BPA (Q. Chen, Lan, Shi, Liu, Zhu, Sun, & Duan, 2019). Due to its vast amount utilised as raw materials in the production of epoxy and polycarbonate resins, BPA pollution is found everywhere, water, soil and air. BPA sources are mostly traced from either wastes gotten from its production, transports and processing or waste from BPA-based products, waste water, and environmental breakdown of plastics (Reddy, Kim, Kavitha, Kumar, Raza, & Kalagara, 2018).

Due to the growing scarcity of freshwater supplies, reclaimed water is an alternative water resource commonly used for irrigation. Still, it may become an

essential source of BPA contamination for food crops and groundwater (Gonzales-Gustavson, Rusiñol, Medema, Calvo, & Girones, 2019).

BPA has also been associated with fissure sealants and composite materials in a dental context where its existence is likely due to impurity from the manufacturing process. BPA is used as a raw material to synthesise many resin monomers in dentistry (Berge, Lygre, Lie, Lindh, & Björkman, 2019). Since the use of such materials in dental care, increased BPA concentrations in saliva and urine have been shown. In contrast, other materials do not offer BPA leaching, suggesting that BPA leaching is material based (Becher, Wellendorf, Sakhi, Samuelsen, Thomsen, Bølling, & Kopperud, 2018). People are subjected to BPA in their everyday lives due to its wide variety of applications, likely without being aware of it.

### **1.2.3(b) Toxicity of BPA**

In humans and animals, exposure to this chemical occurs mainly via the oral (approximately 90 %), gastrointestinal, and dermal routes (Amjad, Rahman, & Pang, 2020; Encarnação, Pais, Campos, & Burrows, 2019). In humans, terrestrial and aquatic animals, BPA exposure has been linked to diabetes, cardiovascular disease, breast cancer, brain development abnormalities, hypertension, obesity, thyroid dysfunction, infertility, and other health problems (Amjad et al., 2020). Many mechanisms, including oxidative stress, affect endocrine and reproductive organs and the immune and central nervous systems (M. S. Rahman, Kang, Arifuzzaman, Pang, Ryu, Song, Park, & Pang, 2019). Oxidative stress refers to the body's imbalance between oxidation and antioxidation, in which oxidation predominates, leading to inflammatory invasion of neutrophils, increased secretion of proteases, and the development of several oxidative intermediates (K. Wang, Zhao, & Ji, 2019). BPA

can cause oxidative stress by entering the body and creating high reactive oxygen species (ROS), causing biological macromolecules to be destroyed, facilitating the production of oxygen-free radicals and raises the amount of oxidative stress in the body or cells and the consequence of the degree of antioxidant gene expression directly or indirectly decreases the antioxidant enzymes and results in oxidative damage to the body by the impaired antioxidant system of biological organisms (X. Zhang & Liu, 2018).

### **1.2.3(b)(i) Toxicity of BPA in Animals**

Growing evidence from laboratory animal studies reveal the toxic effects of BPA on animals and indicates that BPA changes the reproductive function of males and females even at extremely low exposure levels (Vandenberg, Hunt, & Gore, 2019). In a study, adult male Wistar rats were exposed to BPA to investigate the role of gallic acid (GA), a recognised antioxidant, in rat testicular oxidative stress induced by BPA. In this study, the activity of antioxidant enzymes in rats was significantly reduced by BPA and a substantial increase in the levels of reactive oxygen species (ROS) (Olukole, Ola-Davies, Lanipekun, & Oke, 2020). BPA uptake was reported to damage the oxidant-antioxidant equilibrium in mouse colons and livers by causing oxidative stress and lowering antioxidant activity, as seen in Figure 1.3 (K. Wang et al., 2019).

The toxic effect of BPA on porcine embryonic growth was addressed in another report. Increased ROS levels resulting in oxidative stress were triggered by BPA exposure to embryos. Mitochondrial and DNA damage is caused by oxidative stress, which contributes to autophagy (cell degradation). Furthermore, BPA exposure can cause alterations in DNA methylation that may affect the health of

offspring (J. Guo, Zhao, Shin, Niu, Ahn, Kim, & Cui, 2017). The BPA was found to cause damage in the brain, kidney, liver, epididymal sperm and other organs in rodents. It also causes structural changes and many enzymes and receptor protein to not function well in cell signaling. The BPA causes damage to DNA, deformities, and genotoxicity in the liver of mice and rats. Early exposure to BPA during developmental stages could lead to changes in nonhuman primates' mitochondrial activity, thereby causing disease evolution later in life. The degree of toxicity of BPA depends on the dose, exposure age, frequency of exposure and individual differences (Kourouma, Quan, Duan, Qi, Yu, Wang, & Yang, 2015). In another report, an increase in doses of BPA increases immature spermatozoa in rats. A dose of 10 mg/kg of BPA in adult male rats aggravates the vulnerability of its prostate gland to develop hormonal carcinogenesis, reduction in sperm counts and testosterone hence a great fertility consequence. As for neonatal mice, the effects of BPA exposure depend on the amount administered. BPA exposure to neonatal mice could affect the framework of its brain, sexual dimorphism and adult neuronal phenotypes (Mas, Egado, & González-Parra, 2017).

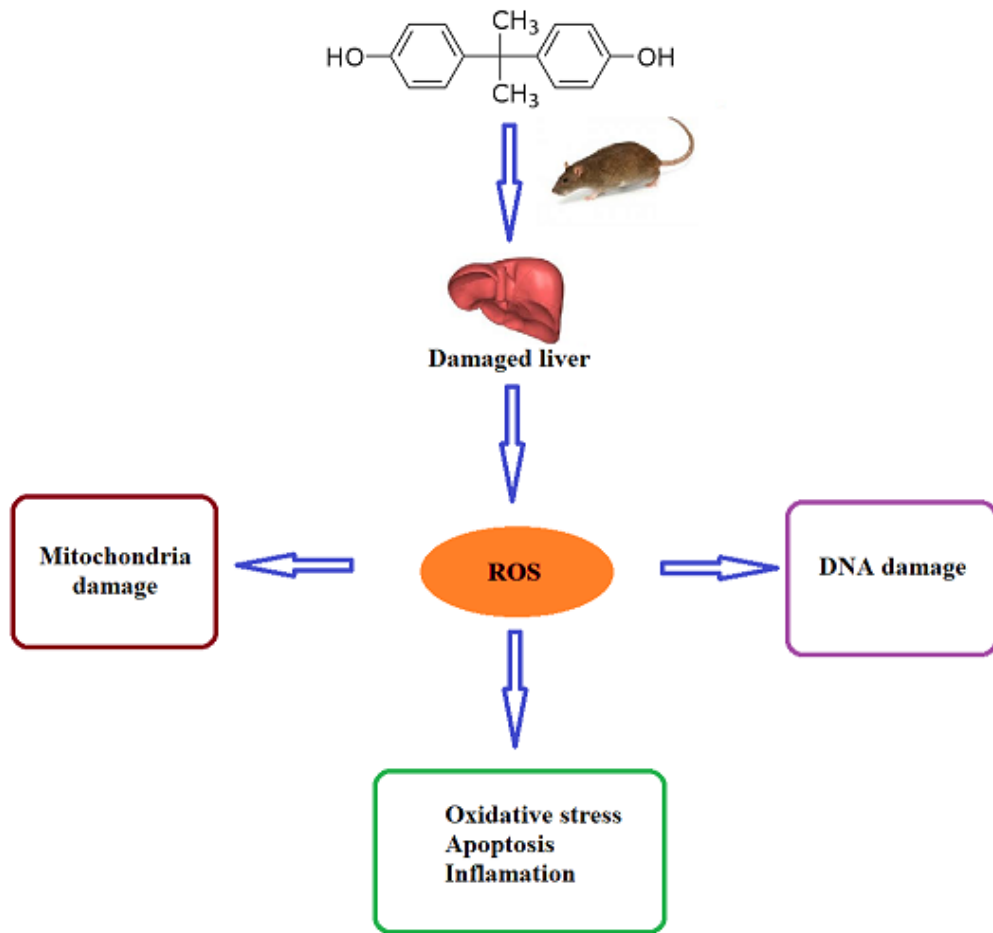


Figure 1.3 Schematic diagram of an adverse effect of BPA

Water polluted with BPA has been reported to instigate histopathological changes in fish. The first organ to be affected is its gills because it is responsible for respiration, osmoregulation and excreting nitrogenous waste products. The histopathological abnormality in gills depends on how long the fish get exposed to BPA. Exposure to BPA may also cause fish to be traumatized, leading to rupture of lamellar capillary and bleeding (Mohammed, Elshaer, Khalaf-Allah, & Bakry, 2013). Fish have been reported to be exposed to BPA via the gills (respiration), leading to estrogenic effects, hence inducing egg yolk protein precursor vitellogenin in male

fishes (Canesi & Fabbri, 2015). In the aquatic environs, marine species react in different ways depending on the concentration of BPA. Table 1.1 lists the effects of BPA doses on different aquatic species.

Table 1.1 Toxicity of BPA on aquatic species

<b>Aquatic species</b>	<b>BPA Dose</b>	<b>Mechanism of Action</b>	<b>Ref.</b>
Frog ( <i>Siluranatropicali</i> )	2.3 $\mu\text{g L}^{-1}$	Inhibition of metamorphosis	(Kashiwagi, Utsumi, Kashiwagi, Ohta, Sugihara, Hanada, & Kitamura, 2008)
Swordtail fish	7 $\mu\text{g L}^{-1}$	Reduced tail length	(Kwak, Bae, Lee, Lee, Lee, Kang, Chae, Sung, Shin, Kim, Mar, Sheen, & Cho, 2001)
Zebrafish	0.2 - 2.2 $\mu\text{g L}^{-1}$	Reduced sperm	(J. Chen, Saili, Liu, Li, Zhao, Jia, Bai, Tanguay, Dong, & Huang, 2017)
Freshwater Ramshorn snail	>1.0 $\mu\text{g L}^{-1}$	Super feminization, oviduct rupture and mortality	(Flint, Markle, Thompson, & Wallace, 2012)
Zebrafish embryos	22 $\text{mg L}^{-1}$ - 6.8 $\text{mg L}^{-1}$	DNA methylation	(Olsvik, Whatmore, Penglase, Skjærven, D'Auriac, & Ellingsen, 2019)
Seahorse ( <i>Hippocampus erectus</i> )	10, 100, and 1000 $\mu\text{g L}^{-1}$	Ovarian failure, apoptosis of follicular cells, and reproductive dysfunction	(Y. Liu, Wu, Qin, Chen, Wang, & Lin, 2021)
Catfish	- 0.05 $\mu\text{g L}^{-1}$ - 2.76 $\mu\text{g L}^{-1}$	- Elevated serum - Cholesterol level	(Makinwa & Uadia, 2017)
Nile tilapia	0.0, 1.64, or 3.28 $\mu\text{g L}^{-1}$	Liver and kidney dysfunction	(Abdel-Tawwab & Hamed, 2018)
Gobiocypris rarus (Fish)	15 $\mu\text{g L}^{-1}$	Disrupted the integrity of Sertoli cell barrier	(S. Tao, Wang, Zhu, Liu, Wu, Yuan, Zhang, & Wang, 2019)
Oyster	2 $\text{mg L}^{-1}$	Affects gonadal development	(L. Luo, Zhang, Kong, Huang, & Ke, 2017)

### **1.2.3(b)(ii) Toxicity of BPA to human**

The BPA is believed to cause endocrine disruption in humans by interacting with a variety of biological receptors, including the androgen receptor (AR), estrogen receptor (ER), and thyroid hormone receptor (THR). As a result of these disrupting effects, there are health risks to the reproductive system, nervous system, metabolic function, immune function, and offspring's growth and development (Ma, Liu, Wu, Yuan, Wang, Du, Wang, Marwa, Petlulu, Chen, & Zhang, 2019). The presence of BPA in human has been detected in urine, plasma, saliva, semen, breast milk, serum, and adipose tissues. Low concentration of BPA was found to have a detrimental effect in humans mostly concerning human development, metabolic activities, reproduction and inflammatory pathways (Usman & Ahmad, 2016; Valentino, D'Esposito, Ariemma, Cimmino, Beguinot, & Formisano, 2016)

Humans are being subjected to BPA levels in different amounts (0.27–10.6 ng/ml) either directly or indirectly. The global BPA intake from dermal exposure, dust inhalation, and ingestion was estimated at 30.76 ng/kg per body weight per day. In humans, the most common route of BPA exposure is through ingestion, which accounts for about 90% of BPA exposures (Ohore & Songhe, 2019). The consequences are numerous, with hormonal abnormalities being the most commonly reported. BPA has been linked to the onset of sexual characteristics and obesity at a young age (Supornsilchai, Jantararat, Nosoognoen, Pornkunwilai, Wacharasindhu, & Soder, 2016). Exposure to high BPA serum concentrations (1.53–2.22  $\mu\text{g L}^{-1}$ ) in males, particularly during the stage of development, male foetuses were feminised as a result, testicular and epididymal atrophy, sperm parameter changes, and testosterone levels reduction (Castellini, Totaro, Parisi, D'Andrea, Lucente, Cordeschi, Francavilla, Francavilla, & Barbonetti, 2020; Karnam, Ghosh, Mondal, &



Mondal, 2015). According to an epidemiological report, men exposed to BPA have a higher risk of low sperm quality than men who are not exposed to BPA. Increased urinary BPA levels were related to reducing sperm concentration, total sperm count, sperm viability, and motility in particular (Cariati, D'Uonno, Borrillo, Iervolino, Galdiero, & Tomaiuolo, 2019). In females, high BPA serum concentrations (1.53–2.22 µg/L) cause changes in estradiol E2, causing hormonal imbalance and anomalies in metabolism such as menstrual irregularities, puberty in its early stages, increased endometriosis risk, Implant failure is more common., and ineffective gonadotropin fertility treatment (Ohore & Songhe, 2019).

Breast milk is an essential source of nutrition for babies. For several years, the World Health Organization (WHO) has advocated for exclusive breastfeeding for the first six months of a baby's life as the best way to provide nutrition (Nasser, Omer, Al-Lenqawi, Al-Awwa, Khan, El-Heneidy, Kurdi, & Al-Jayyousi, 2018). BPA can accumulate in the mammary glands' fat and be ingested by babies during breastfeeding because of its lipophilic properties. For exclusively breastfed infants (0–6 months), the mean amount of BPA was calculated to be 0.3 µg/kg body weight per day, which decreased after the introduction of solid foods (Ma et al., 2019). The BPA can get through the blood-brain barrier (BBB), causing deformity in the central and peripheral nervous system, thereby causing abnormalities in humans (Guida, Troisi, Ciccone, Granozio, Cosimato, Sardo, Ferrara, Guida, Nappi, Zullo, & Di Carlo, 2015).

Drinking water and having access to it is a very important issue for the human population. Water gets contaminated before getting to its consumers through different ways; the source, purification process, leakages, and distribution system (Shaikh, Al Suhaimi, Hanafiah, Ashraf, & Harun, 2018). Different materials are used

in lining the distribution system for water which could further contaminate water through corrosion or leaching, before getting to the consumer. Organic polymers such as epoxy resins and polyurethane are used in lining the pipes to prevent corrosion. Epoxy resins contain BPA and epichlorhydrin; these two components react to form different polymers that leach into drinking water (Rajasärkkä, Pernica, Kuta, Lašňák, Šimek, & Bláha, 2016).

#### **1.2.4 Advanced Oxidation Processes for BPA Removal**

Since BPA is highly soluble in water ( $300 \text{ mg L}^{-1}$  at  $25 \text{ }^\circ\text{C}$ ), it has been found in natural water and wastewater at concentrations ranging from  $1.3$  to  $370 \text{ mg L}^{-1}$ , inland fill leachates as high as  $17 \text{ mg L}^{-1}$ , and sewage sludges, sediment, and biosolids as high as  $95 \text{ mg kg}^{-1}$  (Jhones dos Santos, Sirés, & Brillas, 2021). It is then essential to build technologies to remove BPA in aqueous effluents in order to prevent its harmful effects.

Physical and chemical technologies for pretreatment and treatment of BPA removal have recently been offered. Adsorption, membrane filtration, and a variety of other useful methods for BPA oxidation are among the choices currently available in the removal process. While it is still debatable if these technologies are cost-effective for full-scale plants, their effectiveness is high (Zielinska, Wojnowska-Baryla, & Cydzik-Kwiatkowska, 2018). Significant attempts have been made in recent years to improve advanced treatment to allow for the effective treatment of wastewater to meet strict discharge quality requirements (X. Tian, Song, Shen, Zhou, Wang, Jin, Han, & Liu, 2020). Therefore, advanced oxidation processes (AOPs) such as photocatalysis, will oxidize BPA since various researchers have also looked into it (Kang, Kim, Kim, & Zoh, 2020).

Advanced oxidation processes (AOPs) are water and wastewater treatment methods that use in-situ generated hydroxyl to degrade organic contaminants in the aqueous medium. Because of the superior oxidation capacity of the hydroxyl radical high redox potential ( $E^\circ(\cdot\text{OH}/\text{H}_2\text{O})= 2.8 \text{ V}$ ), hydroxyl radical-based AOPs are the most popular and commonly accepted (Kang et al., 2020); thus AOPs have been commonly used for the degradation of recalcitrant organic pollutants. Hydroxyl radicals are the most common reactive species and a non-selective strong oxidant that is produced in traditional AOPs. They are crucial in the decomposition of organic pollutants that are resistant to degradation. Other reactive species, such as superoxide radicals, can be formed in AOPs in addition to hydroxyl radicals (J. Wang & Wang, 2018). Once generated, hydroxyl radicals can attack organic chemicals through electron transfer, hydrogen abstraction, and radical combination (Mayyahi & Al-asadi, 2018).

Some reactive species, such as singlet oxygen and superoxide radicals, have a lower redox potential than hydroxyl radicals, but they can still degrade certain stubborn organic pollutants (Cai, Li, Xie, Huang, Zeng, Zhang, Liu, Lv, & Liu, 2019). Since reactive species are in charge of degrading organic pollutants in AOPs, understanding the formation, detection, and reaction mechanism of reactive species in various AOPs is critical for understanding the concepts of AOPs and the degradation mechanism of recalcitrant organic contaminants (J. Wang & Wang, 2020). One of the possible classifications for AOPs is dependent on the source of oxidizing species generation, or the process for producing hydroxyl radicals. These are Fenton oxidation, photocatalysis oxidation, electrochemical oxidation, ozonation, gamma-ray/electron beam emission, persulfate-based oxidation, wet air oxidation,